Unusual Metal Ion Catalysis in an Acyl-Transferase Ribozyme†

Hiroaki Suga,*,⊥ James A. Cowan,‡ and Jack W. Szostak*,§

Department of Molecular Biology, Massachusetts General Hospital, Boston, Massachusetts 02114, Department of Chemistry, State University of New York at Buffalo, 657 Natural Sciences Complex, Buffalo, New York 14260-3000, and Department of Chemistry, The Ohio State University, Columbus, Ohio 43210

Received February 24, 1998; Revised Manuscript Received April 30, 1998

ABSTRACT: Most studies of the roles of catalytic metal ions in ribozymes have focused on inner-sphere coordination of the divalent metal ions to the substrate or ribozyme. However, divalent metal ions are strongly hydrated in water, and some proteinenzymes, such as *Escherichia coli* RNase H and exonuclease III, are known to use metal cofactors in their fully hydrated form [Duffy, T. H., and Nowak, T. (1985) *Biochemistry 24*, 1152−1160; Jou, R., and Cowan, J. A. (1991) *J. Am. Chem. Soc. 113*, 6685−6686]. It is therefore important to consider the possibility of outer-sphere coordination of catalytic metal ions in ribozymes. We have used an exchange−inert metal complex, cobalt hexaammine, to show that the catalytic metal ion in an acyl-transferase ribozyme acts through outer-sphere coordination. Our studies provide an example of a fully hydrated Mg^{2+} ion that plays an essential role in ribozyme catalysis. Kinetic studies of wild-type and mutant ribozymes suggest that a pair of tandem G:U wobble base pairs adjacent to the reactive center constitute the metal-binding site. This result is consistent with recent crystallographic studies [Cate, J. H., and Doudna, J. A. (1996) *Structure 4*, 1221−1229; Cate, J. H., Gooding, A. R., Podell, E., Zhou, K., Golden, B. L., Kundrot, C. E., Cech, T. R., and Doudna, J. A. (1996) *Science 273*, 1678−1685; Cate, J. H., Hanna, R. L., and Doudna, J. A. (1997) *Nat. Struct. Biol. 4*, 553−558] showing that tandem wobble base pairs are good binding sites for metal hexaammines. We propose a model in which the catalytic metal ion is bound in the major groove of the tandem wobble base pairs, is precisely positioned by the ribozyme within the active site, and stabilizes the developing oxyanion in the transition state. Our results may have significant implications for understanding the mechanism of protein synthesis [Noller, H. F., Hoffarth, V., and Zimniak, L. (1992) *Science 256*, 1416−1419].

All known natural ribozymes catalyze primarily trans-esterification reactions of phosphodiester bonds. In vitro selection from pools of random RNA sequences has led to the isolation of new ribozymes that catalyze a variety of chemical reactions (*7*, *8*). We have recently used this technique to isolate a novel ribozyme with acyl transfer capability (*9*). This ribozyme is able to efficiently transfer a biotinyl-methionyl group from the 3′-end of a donor hexanucleotide to a hydroxyl or amino group acceptor at its own 5′-end, generating either an ester or amide-linked product, respectively (Figure 1). It can also carry out a multiple turnover trans-esterification reaction and can therefore act as a true enzyme (H. Suga, and J. W. Szostak, manuscript in preparation). In view of the importance of acyl-transfer reactions in biology (*6*) and the likely importance of ribozymes in the evolution of early metabolism and peptide synthesis (*10*), we have begun to dissect the mechanism of catalysis of acyl-transfer by this ribozyme.

Most ribozymes are considered to be metalloenzymes, in which divalent metal ions play critical catalytic roles (*11*, *12*). A strategically positioned metal ion is directly (*inner-sphere*) coordinated to a substrate atom, so as to assist in deprotonation of the attacking nucleophile, stabilization of the leaving group, or stabilization of the transition state. Elegant support for this model has been obtained in several cases by the kinetic studies of ribozymes (*13*−*27*). In the case of the hammerhead ribozyme, for instance, the bound metal ion acts to decrease the pK_a of the attacking 2′-hydroxyl; activity is directly proportional to the K_a of the metal-bound water (*14*). In the case of *Tetrahymena* ribozyme, Mn^{2+} can rescue the deleterious effects of a thio-

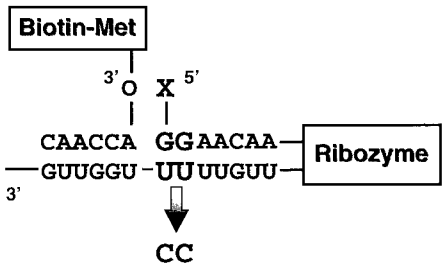

FIGURE 1: Schematic of the acyl-transferase ribozyme. The substrate, a hexanucleotide (5′-CAACCA) carrying a biotinylated methionine at its 3′-end, binds to a complementary sequence located near the 3′-end of the ribozyme. The biotinyl-methionyl group is transferred to the 5′-hydroxyl (X = OH) or 5′-amino (X = NH_2) group of the ribozyme to form an ester or amide-linked product, respectively. A mutant ribozyme (UU → CC) forms two G:C Watson−Crick base pairs instead of G:U wobble base pairs.

† This research was supported by NIH Grant R01 GM53936 to J.W.S. and SUNY at Buffalo Startup Funds to H.S.

* Author to whom correspondence should be addressed. E-mail: hsuga@acsu.buffalo.edu.

⊥ State University of New York at Buffalo.

‡ The Ohio State University.

§ Massachusetts General Hospital.

S0006-2960(98)00432-2 CCC: $15.00
Published on Web 06/24/1998

substitution for the bridging 3′-oxygen of phosphodiester linkage at the cleavage site, in which the oxygen is normally coordinated to Mg^{2+} (*17*).

Although the above chemical mechanism is generally accepted in the ribozymes that have been studied to date, it is likely that other mechanisms could operate in ribozyme catalysis. Recent studies of the hairpin ribozyme indicate that neither direct binding of metal ions to phosphate oxygens nor nucleophilic activation of metal-bound water are required for activity (*28*, *29*). Instead, the critical metal ions required for structure formation or for catalysis are likely to interact with the RNA through outer-sphere coordination. Here, we report mechanistic studies of the acyl-transferase ribozyme focused on the catalytic role of divalent metal ions. A single catalytic metal ion bound to a specific site on the ribozyme appears to play a critical role in stabilizing the transition state through outer-sphere coordination.

MATERIALS AND METHODS

Materials. Buffers and salts were purchased from Sigma. NTPs and dNTPs were purchased from Pharmacia. [α-^{32}P]-UTP[1] was purchased from DuPont-New England Nuclear. T7 RNA polymerase was purified from an overproducing strain. Taq polymerase was purchased from Boehringer Mannheim. RNase free DNase and calf intestinal phosphatase were purchased from New England Bio-Labs. 5′-Amino guanosine was chemically synthesized and HPLC purified (J. Lorsh, P. A. Lohse., and J. W. Szostak, unpublished). The acyl hexanucleotide was chemically synthesized and HPLC purified (*30*). Synthesis of *N*-biotinyl-methionyl hexanucleotide was reported elsewhere (*30*).

Ribozyme Synthesis. Ribozymes were synthesized by T7 RNA polymerase runoff transcription of PCR DNA templates (clone E18) in the presence of [α-^{32}P]UTP. For the mutant ribozyme, WC18, the DNA template coding for E18 was amplified by PCR in the presence of appropriate primers to introduce the mutations. The PCR was carried out for 20 productive cycles to ensure that the amplified DNA would contain less than 0.001% of the original DNA template. The transcripts were treated with RNase-free DNase for 30 min. Products were purified by denaturing polyacrylamide gel electrophoresis and were passively eluted from the gel into 0.3 M NaCl. The ethanol-precipitated RNA was dephosphorylated by treatment with calf intestinal phosphatase for 1 h, and the product was isolated by phenol-chloroform extraction, ethanol precipitation, resuspended in distilled water, and stored at −20 °C.

General Kinetics. Reactions were carried out as follows. A total of 48 μL of a ribozyme solution was prepared by mixing of 6 μL of 300 nM ribozyme with 15 μL of 4× buffer (400 mM KCl and 100 mM HEPES, pH 8.0) and 27 μL of water, heating at 90 °C for 5 min, and then transferred to 25 °C, where it remained for 5 min. To this solution was added 6 μL of 100 mM divalent metal, and the mixture was incubated for 5 min. Reactions were initiated by the addition of 6 μL of 10 μM substrate to the ribozyme solution and incubated for various times. Reactions were stopped by adding 6 μL of the reaction mixture to 3 μL of quenching buffer containing 8 M urea, 70 mM EDTA, 42 μM streptavidin, and 50 mM Tris·HCl adjusted to pH 6.0 (*31*). Samples were subjected to electrophoresis on 6% polyacrylamide, 8 M urea gels running in a cold room to keep the gel temperature below 30 °C. Gels were exposed to a phosphor storage screen (Molecular Dynamics) for 5−24 h and were quantified using a phosphorimager. Data were analyzed using the KaleidaGraph graphing and curve-fitting package (Abelbeck Software). Velocities were determined by taking at least five points from the linear regions of the time course. The yield of 5′-acylated ribozyme (X = OH) reached a plateau at approximately 50%, suggesting that only half of the ribozyme was active, probably due to the incorrect folding. Catalytic constants were corrected to reflect 50% functional ribozyme concentration (*9*). The reported rate constants are the average of rates from 2 to 3 kinetic experiments.

Synthesis of 5′-NH$_2$ Ribozyme. The 5′-NH$_2$ ribozyme was prepared by T7 RNA polymerase runoff transcription of the E18 DNA template under the following conditions: buffer (40 mM CHES adjusted to pH 9.0, 35 mM $MgCl_2$, 1 mM spermidine, 0.01% Triton X-100, and 10 mM DTT), 1 mM each of ATP, UTP, and CTP, 0.1 mM GTP, 2.5 mM 5′-amino-guanosine, and [α-^{32}P]UTP. The transcripts were treated with RNase-free DNase and purified by denaturing polyacrylamide gel electrophoresis. The products were eluted from the gel in 0.3 M NaCl and precipitated with ethanol. Since GTP-primed (5′-ppp) ribozyme is inactive, the fraction of active 5′-NH$_2$ ribozyme was estimated by incubating transcripts (40 nM) with 1 μM substrate under reaction conditions for 1 h, which allowed complete acylation of the 5′-NH$_2$ group. The yield of 5′-acylated ribozyme (X = NH$_2$) reached a plateau at approximately 20%. Catalytic constants for the 5′-NH$_2$ ribozyme were corrected to reflect 20% functional ribozyme concentration.

Metal Titration Experiments. Metal(II) chloride was dissolved in water to prepare a 0.5 M stock solution. Metal-(III) hexammine was disolved in water containing 1 mM EDTA to prepare a 0.1 M stock solution and was stored at −20 °C. A total of 42 μL of a ribozyme solution was prepared by mixing 6 μL of 300 nM ribozyme with 15 μL of 4× buffer (400 mM KCl and 100 mM HEPES, pH 8.0) and 27 μL of water, heating at 90 °C for 5 min, and cooling to 25 °C for 5 min. To this solution was added 6 μL of 10 mM spermidine (or water) and 6 μL of divalent metal ion solution, and the mixture was incubated for 5 min. Reactions were initiated by the addition of 6 μL of 10 μM substrate to the ribozyme solution and incubated for various times. We also performed the final substrate concentration at 2 μM instead of 1 μM for each metal ion tested, which gave virtually the same results. Thus, under these conditions, the ribozyme is saturated with the substrate (K_m = 124 nM) so that the observed rate constants (k_{obs}) should approximate the maximal value (k_{cat}) at each concentration of metal ion tested. In the case of high concentrations of metal ion (above 100 mM), the volume of water was reduced to adjust the

[1] Abbreviations: Biotin-Met, biotinyl-methionyl; HEPES, *N*-(2-hydroxylethyl)piperazine-*N*′-(2-ethanesulfonic acid); K_d, equilibrium dissociation constant; k_{obs}, observed catalytic constant; k_{obs}^{max}, maximal observed catalytic constant; k_{obs}^{H2O}, observed catalytic constant in water; k_{obs}^{D2O}, observed catalytic constant in deuterium oxide; NTPs, ribonucleotides triphosphate; dNTPs deoxyribonucleotides triphosphate; PIPES, piperazine-*N*,*N*′-bis(2-ethanesulfonic acid); Ribz, acyl-transferase ribozyme; SAv, Streptavidin; UTP, uridine triphosphate.

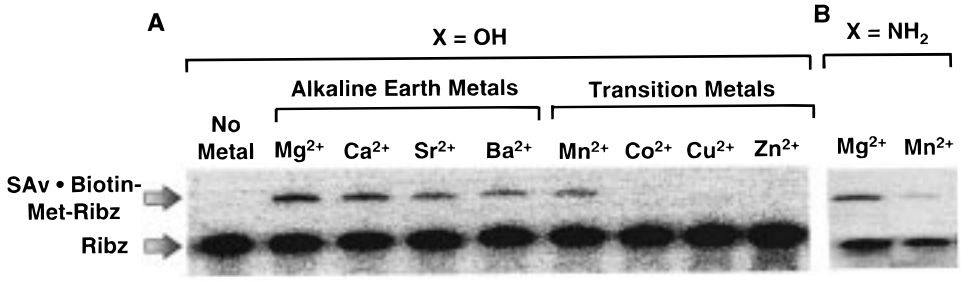

FIGURE 2: Divalent metal ion dependence of the acyl-transfer reaction catalyzed by the ribozyme. (A) X = OH and (B) X = NH_2. Reactions were carried out in the presence of 10 mM divalent metal ion, in 100 mM KCl and 25 mM HEPES, pH 8.0, for 2 min (A) or 10 min (B). Streptavidin (SAv) binds to the biotin attached to the methionyl group (Biotin-Met) and causes a gel mobility shift when the ^{32}P-labeled ribozyme (Ribz) is acylated.

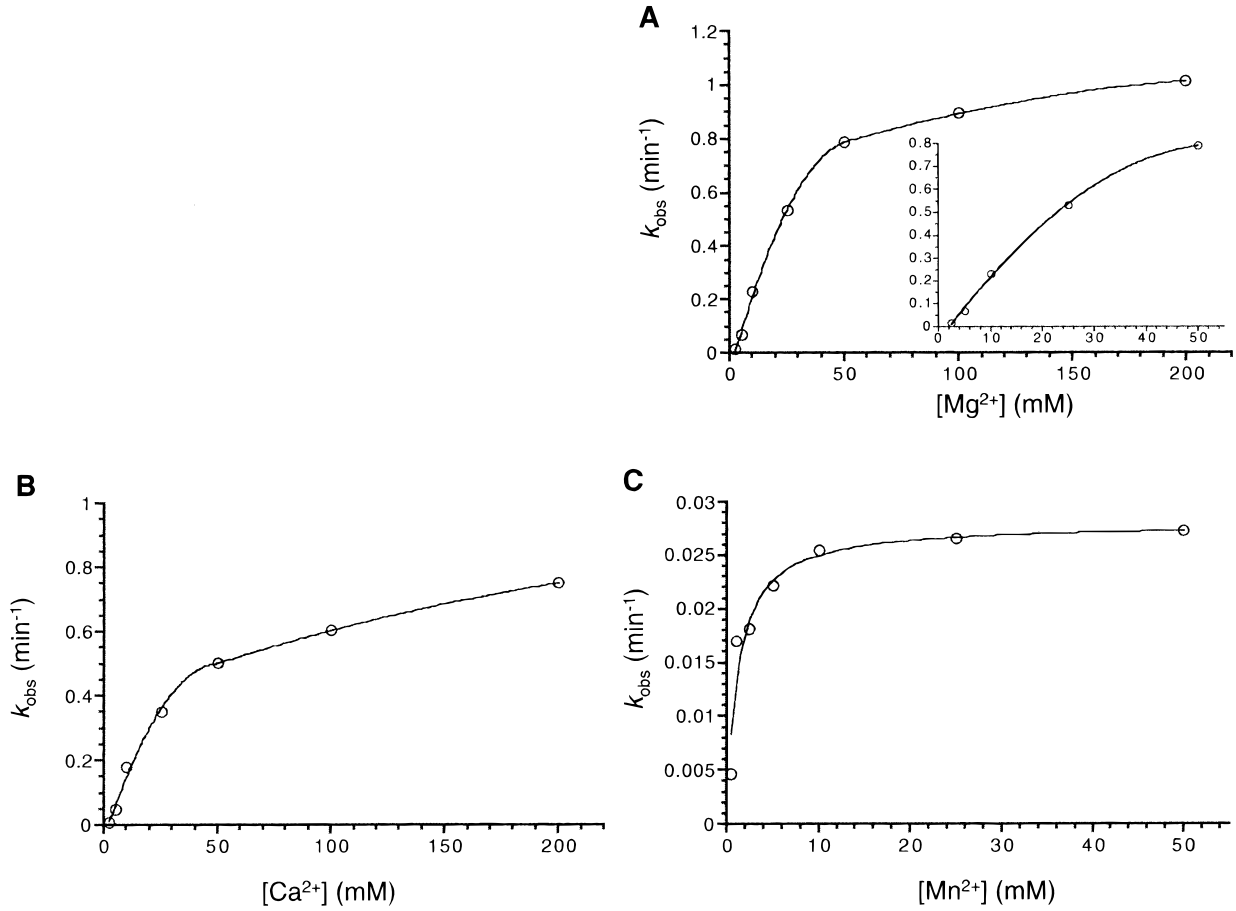

FIGURE 3: Catalytic activity of ribozyme (X = OH) vs divalent metal ion concentration. (A) Mg^{2+} (inset shows activity below 30 mM Mg^{2+}), (B) Ca^{2+}, (C) Mn^{2+}.

metal ion concentration. The remaining procedures were performed as described in general kinetics.

pH-Dependent Kinetics and Solvent Isotope Effects Experiments. Buffers were PIPES (pH 6.0) or HEPES (pH 7.0, 7.5, and 8.0). The pH of each buffer was adjusted with KOH. In the case of D_2O-containing buffer solutions, the pH was adjusted with KOD and was corrected by adding 0.4 to the reading obtained with a glass electrode according to the equation of pH = pD + 0.139α + 0.0854α^2, where α is the atom fraction of deuterium (*32*). Ribozyme, substrate, and metal solution were lyophilized from D_2O prior to use for the experiments. The remaining procedures were performed as described in general kinetics except that a final concentration of 50 mM $MgCl_2$ was used.

RESULTS AND DISCUSSION

Divalent Metal Ion Dependence of Ribozyme Catalysis and Number of Essential Catalytic Metal Ions. To gain insight into the roles of divalent metal ions, we first examined the catalytic activity of the ribozyme in the presence of various metal ions. The acyl-transferase ribozyme, in common with some other known ribozymes (*12*), requires divalent metal ions for catalytic function (Figure 2A). Although the selection was carried out in the presence of Mg^{2+} as the only divalent metal ion, catalytic activity is retained in the presence of various alkaline earth metals. Of the transition metal ions, Mn^{2+} is able to support catalysis, with considerably lower activity than Mg^{2+}, but Co^{2+}, Cu^{2+}, and Zn^{2+} are inactive. The metal-dependent acyl-transfer activity is

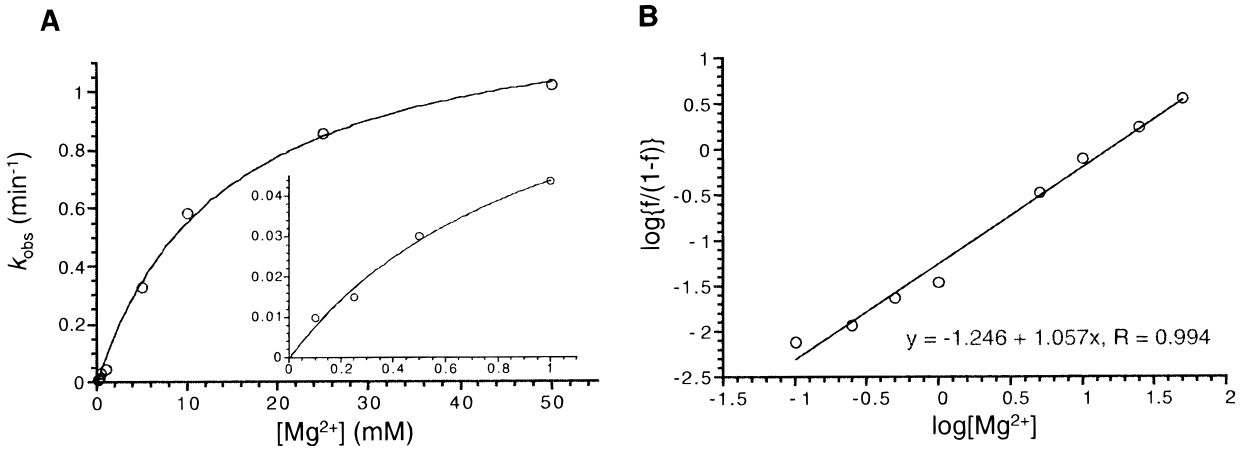

FIGURE 4: Catalytic activity of ribozyme (X = OH) vs Mg^{2+} concentration in the presence of 1 mM spermidine. (A) Inset shows activity below 1 mM Mg^{2+}. Fitting the data to the equation $k_{obs} = k_{obs}^{max}[Mg^{2+}]/(K_d + [Mg^{2+}])$ yielded a K_d and k_{obs}^{max} shown in Table 1. (B) Hill analysis of the data in panel A; *f* represents fraction of activity at saturating Mg^{2+}.

not directly proportional to the K_a of metal-bound water, in contrast to the case of the hammerhead ribozyme, where the observed hydrolytic activity is approximately proportional to the K_a of metal-bound water (*14*). The pK_a of water bound to Mg^{2+}, Ca^{2+}, and Mn^{2+} is 11.4, 12.8, and 10.6, respectively. If catalytic activity directly reflected these values, activity should be greatest in the presence of Mn^{2+}, and least with Ca^{2+}, whereas the observed activity is greatest with Mg^{2+}, slightly less with Ca^{2+}, and least with Mn^{2+}, suggesting that the role of the metal ion is not simply to generate metal-hydroxide ion for the deprotonation of the nucleophile.

Failure of the acyl-transfer activity to follow the pK_a rule for water bound to metal ions could be due to any of several effects, including differential binding of different metal ions, binding of multiple metal ions with different structural and catalytic roles, or changing rate-limiting step with different metal ions. To assess the number of metal ions required for activity, we measured the initial rate as a function of the concentration of Mg^{2+} (Figure 3A). The titration curve is complex, with no observable activity below approximately 1 mM Mg^{2+}, activity rapidly increasing up to 50 mM, and then slowly increasing beyond 50 mM. This observation suggests that more than one Mg^{2+} ion is required for ribozyme activity.

The titration of catalytic activity for Ca^{2+} is similar to that for Mg^{2+} (Figure 3B). Mn^{2+} is the only transition metal ion to support catalysis among others tested, but it exhibits a significantly different metal-ion-dependent behavior (Figure 3C). The catalytic activity observed in the presence of 10 mM Mn^{2+} is approximately 10-fold lower than that in 10 mM Mg^{2+}, consistent with the earlier observation. However, approximately 10 mM of Mn^{2+} completely saturates the activity. This behavior reflects the apparent catalytic activity for 50 mM Mn^{2+}, which is approximately 30-fold lower than that for 50 mM Mg^{2+}.

The catalytic function of ribozymes relies upon the formation of folded structure, which often requires divalent metal ions such as Mg^{2+} (*15*, *33*, *34*). To distinguish between structural and catalytic roles, we attempted to replace structural Mg^{2+} ions with spermidine (*14*, *15*, *23*). The Mg^{2+}-titration data in the presence of 1 mM spermidine fit a simple single-site saturation curve (Figure 4A). The slope of a Hill plot is 1.0 (Figure 4B), suggesting that only one metal ion is required for catalysis, in the presence of spermidine. The Mg^{2+} concentration at the half-maximal rate is 14 mM (Table 1); assuming that the metal ion is in rapid equilibrium with the ribozyme, this should approximate the dissociation constant (K_d) of the metal ion to the ribozyme (Table 1).

Table 1: Dissociation Constants of Metal Ions for Ribozyme (X = OH) and Their Maximal Rate Constants[a]

metal	K_d (mM)	k_{obs}^{max} (min^{-1})
Mg^{2+}	14.0 ± 1.5	1.32 ± 0.05
Ca^{2+}	(12.8 ± 8.9)[a]	(0.633 ± 0.282)[a]
Mn^{2+}	(1.15 ± 0.39)[a]	(0.165 ± 0.030)[a]
$[Co(NH_3)_6]^{3+}$	0.354 ± 0.074	1.00 ± 0.06

[a] Since the parameters are derived from the limited region indicated in Figure 5, they are not determined well.

The Ca^{2+}-titration data in the presence of 1 mM spermidine are similar to the Mg^{2+}-titration data but fit a simple saturation curve only at concentrations below 10 mM (Figure 5A). The apparent K_d from data in this region is approximately 13 mM (Table 1), which is similar to that observed for Mg^{2+}. Above 10 mM, the activity gradually decreases. This behavior is presumably due to the binding of Ca^{2+} to other, unfavorable metal-binding sites in the ribozyme, causing structural perturbations. This tendency was even more pronounced in the Mn^{2+}-titration experiment in the presence of 1 mM spermidine (Figure 5B). While the titration data follow a saturation curve up to 2 mM, the catalytic activity drastically decreases above 2 mM. The derived K_d and maximal rate constant (k_{obs}^{max}) for Mn^{2+} are 1.15 mM and 0.165 min^{-1}, respectively, which are 12-fold and 8-fold lower than those for Mg^{2+}, respectively (Table 1). However, we cannot rule out the possibility that the changes in rate reflect a change in rate-limiting step in the presence of different metal ions, or, in the case of Mn^{2+}, the formation of inhibitory metal polyhydroxide complexes.

pH Dependence and Solvent Isotope Effect of Acyl-Transfer Reaction Catalyzed by Ribozymes. To further test the possible role of the catalytic metal ion as a general base, we measured pH-dependent rate and solvent isotope effects for the ribozyme. The catalytic rate constants (k_{obs}) measured in standard buffered H_2O were plotted as a function of pH (pH vs log k_{obs}, Figure 6A). The rate constants for the 5′-

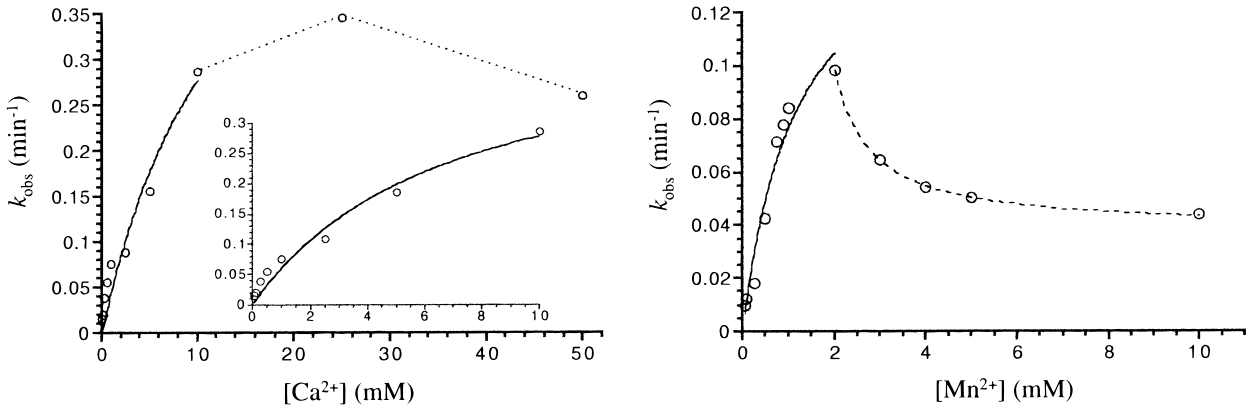

FIGURE 5: Catalytic activity of ribozyme (X = OH) vs Ca^{2+} (A) or Mn^{2+} (B) concentration in the presence of 1 mM spermidine. (A) Inset shows activity below 10 mM Ca^{2+}. Fitting the data in this region to the equation $k_{obs} = k_{obs}^{max}[Ca^{2+}]/(K_d + [Ca^{2+}])$ yielded a K_d and k_{obs}^{max} shown in Table 1. (B) Fitting the data below 2 mM to the equation $k_{obs} = k_{obs}^{max}[Mn^{2+}]/(K_d + [Mn^{2+}])$ yielded a K_d and k_{obs}^{max} shown in Table 1.

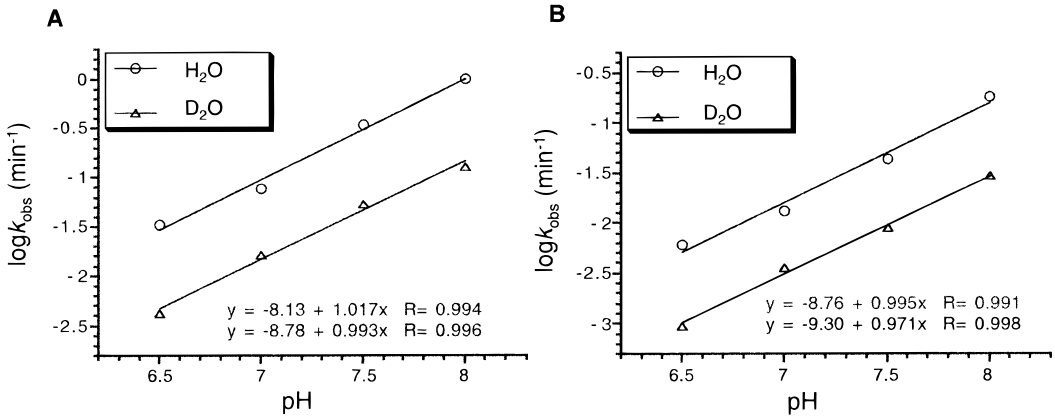

FIGURE 6: pH dependence of 5′-OH (A) and 5′-NH_2. (B) Ribozyme-catalyzed reaction. Reactions are carried out under the conditions described in Materials and Methods.

OH ribozyme linearly increase as the pH values increase, indicating that the reaction is dependent upon the concentration of hydroxide ion. The slope of this plot is approximately 1, suggesting that one rate-limiting ionization occurs during the catalysis. This behavior is similar to that observed in other known ribozymes (*14*, *23*, *35*−*37*), even though the activity of this ribozyme does not obey the pK_a rule for water bound to metal ions. Identical pH-dependent behavior was observed when the reaction was carried out in a D_2O buffer (Figure 6A), except for a large reduction of the catalytic constants observed at each pH (vide infra).

A modified ribozyme carrying a 5′-amino group (X = NH_2) instead of a 5′-hydroxyl group is also capable of catalyzing the acyl-transfer reaction to yield an amide-linked product (Figure 1) (*9*). Heteroatom substitution of the nucleophile or the leaving group is an effective way to determine whether the metal ion(s) interacts with the specific group in the transition state, since it dramatically affects the catalytic parameters if the substituted group is involved in the rate-limiting step. We therefore studied the pH dependence and solvent isotope effects for the 5′-NH_2 ribozyme. A plot of k_{obs} as a function of pH in both H_2O buffer and D_2O buffer reveals a linear correlation between pH and log k_{obs}, and the slope of the both plots is again approximately 1 (Figure 6B). These results suggest that the 5′-OH and 5′-NH_2 ribozymes accelerate the acyl transfer reaction via a common mechanism that does not involve direct interaction of the metal ion with the nucleophile.

This view of the catalytic role of the divalent metal ion is further strengthened by the following experiments. Mn^{2+} binds equally well to oxygen and nitrogen, whereas Mg^{2+} preferentially binds to oxygen over nitrogen (*38*, *39*). If the metal ion were to play a critical role in the generation of the nucleophilic anion, the substitution of a hydroxyl nucleophile by an amine would be expected to alter the metal ion dependence of the ribozyme. The observed activity of the 5′-NH_2 ribozyme is, however, approximately 10-fold greater in the presence of Mg^{2+} than in Mn^{2+}, virtually the same as observed for the 5′-OH ribozyme (Figure 2B). These results again argue against direct metal−nucleophile (i.e., inner-sphere) interactions.

The degree of solvent isotope effect generally reflects the number of proton-transfer events occurring in the rate-limiting step, but can also be influenced by a variety of other factors including conformational changes or factors affecting the protonation/deprotonation of catalytic residues and metal ions (*35*, *40*). The effects observed in the 5′-OH and 5′-NH_2 ribozymes are 7.7- and 6.4-fold, respectively (Table 2). This magnitude is larger than that commonly observed for a single proton transfer in a rate-limiting step, and is also larger than the values previously reported for the hammerhead ribozyme (*18*, *19*, *22*). Although solvent isotope effects are notoriously difficult to interpret, the similarity of the solvent isotope effects observed in both 5′-OH and 5′-NH_2 ribozymes

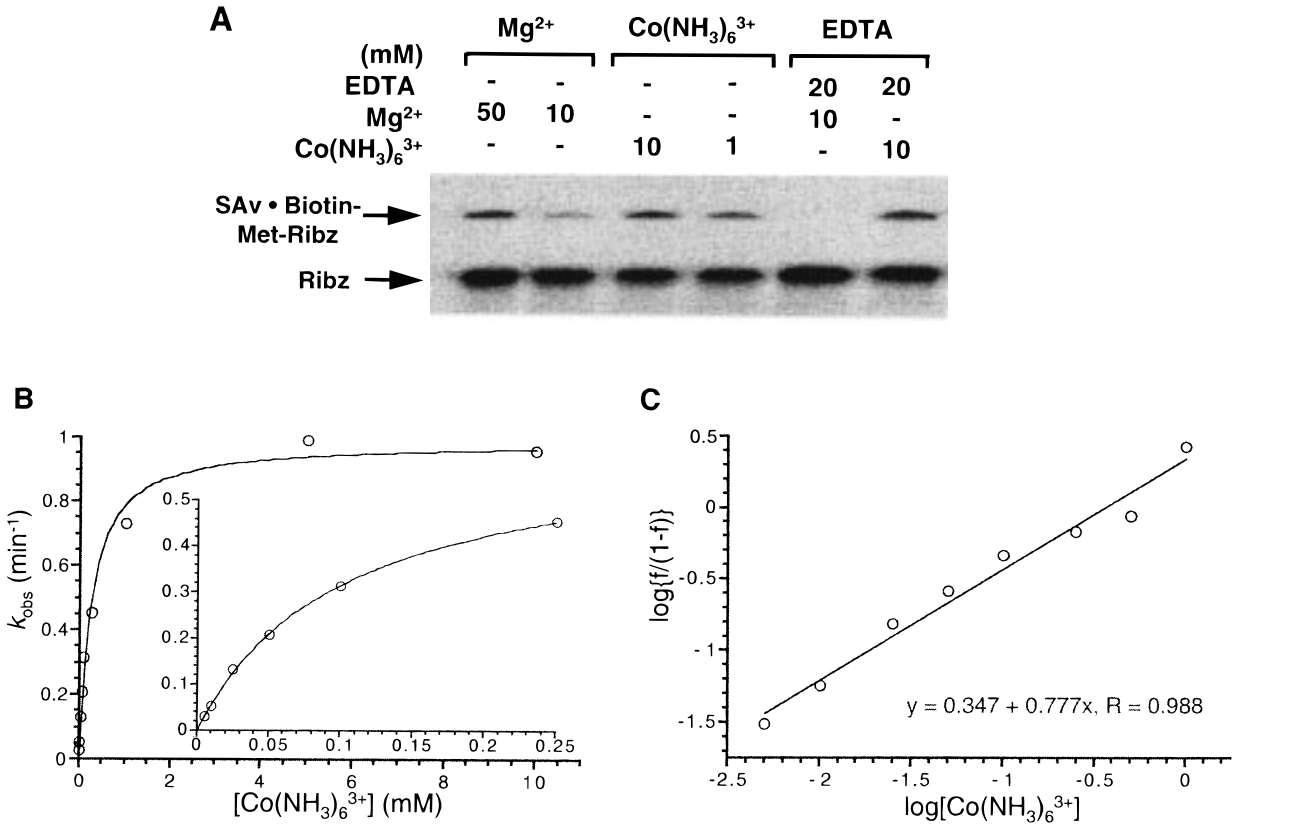

FIGURE 7: (A) Comparison of ribozyme activity in the presence of Mg^{2+} or $Co(NH_3)_6^{3+}$. Reactions were incubated for 1 min at pH 8.0. (B) Catalytic activity of ribozyme (X = OH) vs $Co(NH_3)_6^{3+}$ concentration in the presence of 1 mM spermidine. Inset shows activity below 0.25 mM of $Co(NH_3)_6^{3+}$. Fitting the data to the equation $k_{obs} = k_{obs}^{max}[Co(NH_3)_6^{3+}]/(K_d + [Co(NH_3)_6^{3+}])$ yielded a K_d and k_{obs}^{max} shown in Table 1. (C) Hill analysis of the data in panel B.

Table 2: Solvent Isotope Effects of 5′-OH and 5′-NH_2 Ribozymes

ribozyme	k_{obs}^{H2O} (min^{-1})	k_{obs}^{D2O} (min^{-1})	$k_{obs}^{H2O}/k_{obs}^{D2O}$
5′-OH	1.01 ± 0.025	0.131 ± 0.0018	7.7
5′-NH_2	0.188 ± 0.031	0.0293 ± 0.0065	6.4

is consistent with the view that the mechanism of the ribozyme-catalyzed acyl-transfer reaction is not changed by changing the identity of the nucleophile.

Coordination of the Catalytic Metal Ion. Since the catalytic Mg^{2+} ion did not appear to promote catalysis by altering the pK_a of the nucleophile, we wondered if direct coordination to the substrate or ribozyme was required. We used cobalt(III) hexammine, $Co(NH_3)_6^{3+}$, as a probe for the outer-sphere-mediated effects of Mg^{2+} (Figure 7A), since it has similar size and geometry to $Mg(H_2O)_6^{2+}$ (*2*, *28*, *29*). Its slow ligand exchange rate ($k_{exchange} = 10^{-10}$ s^{-1}) essentially precludes inner-sphere (direct) coordination to functional groups on the ribozyme or substrate (*41*). $Co(NH_3)_6^{3+}$ was able to replace Mg^{2+} in both structural and catalytic roles, resulting in a comparable catalytic rate in the presence of 10 mM $Co(NH_3)_6^{3+}$ or 50 mM Mg^{2+}. The addition of EDTA did not affect the rate of the $Co(NH_3)_6^{3+}$ reaction, while it completely inhibited Mg^{2+}-dependent catalysis. In the presence of spermidine, the $Co(NH_3)_6^{3+}$-titration data fits a single-site saturation curve (Figure 7B), with a K_d of 350 μM (40-fold lower than that observed for Mg^{2+}). The high affinity of $Co(NH_3)_6^{3+}$ for the ribozyme most likely reflects strong electrostatic interactions with the ribozyme. Hill analysis provided a slope of 0.8, which is consistent with a single metal ion participating in catalysis (Figure 7C). These

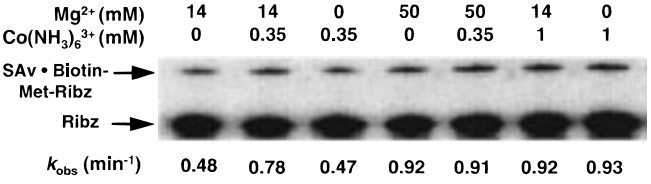

FIGURE 8: Comparison of ribozyme activity in the presence of Mg^{2+} or $Co(NH_3)_6^{3+}$ or both ($t = 15$ s). k_{obs}s were determined as described in Materials and Methods.

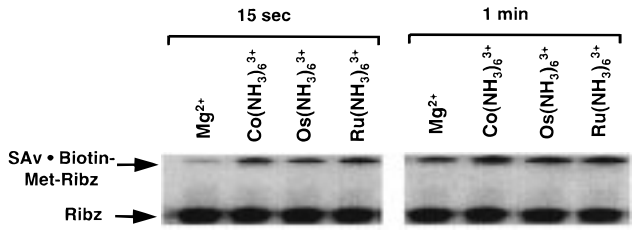

FIGURE 9: Comparison of ribozyme activity in the presence of 10 mM Mg^{2+} or metal(III) hexammine.

results strongly suggest that the essential Mg^{2+} acts in the hydrated form, $Mg(H_2O)_6^{2+}$, to promote the reaction, consistent with its preferred binding mode to structured nucleic acids (*42*, *43*).

To test the possibility that $Co(NH_3)_6^{3+}$ occupies a different binding site from Mg^{2+} and promotes catalysis by a different mechanism, we carried out competition experiments in which either Mg^{2+} or $Co(NH_3)_6^{3+}$ or both were present under subsaturating and saturating conditions (Figure 8). Under subsaturating conditions (where the concentration of metal ion is approximately equal to its K_d), the observed catalytic

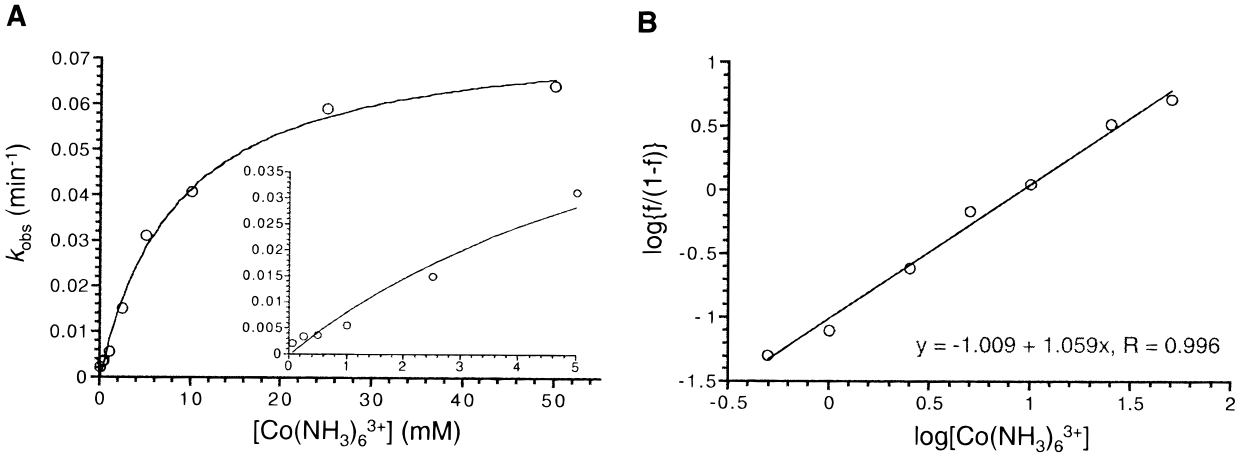

FIGURE 10: (A) $Co(NH_3)_6^{3+}$-titration for catalytic activity of the Watson−Crick mutant ribozyme (X = OH) in the presence of 1 mM spermidine. Inset shows activity below 5 mM $Co(NH_3)_6^{3+}$. Fitting the data to the equation $k_{obs} = k_{obs}^{max}[Co(NH_3)_6^{3+}]/(K_d + [Co(NH_3)_6^{3+}])$ yielded a K_d (8.5 mM) and k_{obs}^{max} (0.077 min^{-1}). (B) Hill analysis of the data in panel A.

rate in the presence of both metal ions is greater (approximately 1.6-fold faster) than that in the presence of either metal ion alone. On the other hand, under saturating conditions, the addition of either metal ion results in neither enhancement nor inhibition of the catalytic rate, consistent with both metal ions occuping the same site on the ribozyme.

Although $Co(NH_3)_6^{3+}$ is kinetically stable and has a slow ligand-exchange rate, it is possible that a slight contamination with degraded $Co(NH_3)_6^{3+}$ could be responsible for the catalytic activity. To rule out this possibility, we also examined catalysis in the presence of $Os(NH_3)_6^{3+}$ or $Ru(NH_3)_6^{3+}$, the latter of which is even more kinetically stable than $Co(NH_3)_6^{3+}$ and is available in high purity. The ribozyme-catalyzed reaction in the presence of either $Os(NH_3)_6^{3+}$ or $Ru(NH_3)_6^{3+}$ proceeds with virtually the same rate as for $Co(NH_3)_6^{3+}$ (Figure 9). This result, in combination with the observation that the $Co(NH_3)_6^{3+}$-promoted reaction is insensitive to EDTA addition (Figure 7A) supports the conclusion that metal hexammine is responsible for the catalytic activity.

Binding Site of the Catalytic Metal Ion. The two 5′-terminal Gs of the ribozyme form tandem G:U wobble base pairs with the internal template region (Figure 1). Mutation of these base pairs to G:C Watson−Crick base pairs diminishes the catalytic rate constant by 20-fold in the presence of Mg^{2+}, while the Michaelis constant for substrate is virtually unchanged (*30*). This suggests a significant catalytic role for the wobble base pairs. We have repeated the $Co(NH_3)_6^{3+}$ titration experiment with the mutant ribozyme in the presence of 1 mM spermidine (Figure 10A). The titration curve shows simple saturation behavior similar to that of the wild-type ribozyme, but the maximal rate achieved by the mutant ribozyme was again 20-fold lower than that for the wild-type ribozyme. Interestingly, the concentration of $Co(NH_3)_6^{3+}$ required to reach the half-maximal rate was 20-fold higher (K_d = 8.5 mM) than for the wild-type ribozyme. Hill analysis again indicates that a single metal ion is required for catalysis (Figure 10B). These results are consistent with the metal-binding site that is being titrated in these experiments being at least partially composed of these wobble base pairs, and therefore located very close to the active site of the ribozyme.

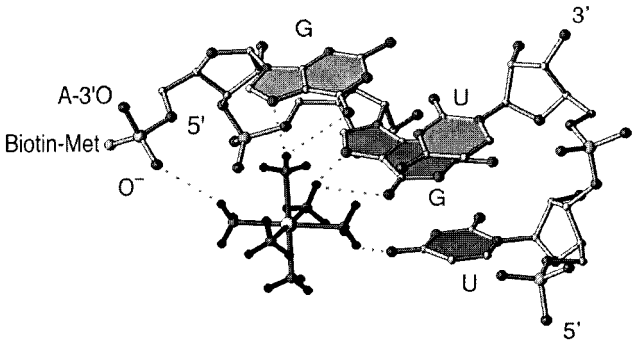

FIGURE 11: Model of transition state of the acyl-transfer reaction catalyzed by ribozyme based on complex observed by Cate and Doudna (*3*). Cobalt(III) hexaammine is shown in the middle; it stabilizes the developing oxyanion (O^-) of the acyl group in the transition state.

Cate and Doudna have recently reported a 2.8 Å crystal structure of the P4−P6 domain of *Tetrahymena thermophila* group I intron (*3*, *4*). They observed that tandem G:U wobble base pairs in the intron structure constitute good binding sites for the hexaammines $Co(NH_3)_6^{3+}$ and $Os(NH_3)_6^{3+}$ and by implication for hydrated Mg^{2+}. Such a metal ion bound in the major groove of adjacent wobble base pairs is positioned very close to a nonbridging oxygen of the 5′-most phosphate of the sequence 5′-pGpG-3′. The tetrahedral transition state for the acyl-transfer reaction resembles a phosphate moiety and would be located at a position nearly identical to this 5′-phosphate. These results have led us to a model in which $Co(NH_3)_6^{3+}$ [or $Mg(H_2O)_6^{2+}$] bound in the major groove of the tandem G:U wobble base pairs stabilizes the developing negative charge of the oxyanion in the transition state (Figure 11). We propose that the role of the rest of the ribozyme is to help to precisely position the bound metal ion near the oxyanion in the transition state. Further experiments are now being carried out to address this and alternative models.

In summary, we have presented evidence that the catalytic metal ion in an acyl-transferase ribozyme acts through outer-sphere coordination to the substrate and ribozyme. Our findings expand the diversity of chemical mechanisms known to be used by ribozymes. Since the chemistry of the acyl-transfer reaction is the same as that of peptidyl-transfer, we

suggest that a similar mechanism could operate in the peptidyl transferase center of the ribosome (*6*).

ACKNOWLEDGMENT

We thank Dr. Jamie Cate for his generous assistance with the preparation of Figure 11 and gift of $Os(NH_3)_6^{3+}$. We also thank Drs. Peter Lohse, David Huizenga, and David Wilson for helpful discussions.

REFERENCES

1. Duffy, T. H., and Nowak, T. (1985) *Biochemistry 24*, 1152−1160.
2. Jou, R., and Cowan, J. A. (1991) *J. Am. Chem. Soc. 113*, 6685−6686.
3. Cate, J. H., and Doudna, J. A. (1996) *Structure 4*, 1221−1229.
4. Cate, J. H., Gooding, A. R., Podell, E., Zhou, K., Golden, B. L., Kundrot, C. E., Cech, T. R., and Doudna, J. A. (1996) *Science 273*, 1678−1685.
5. Cate, J. H., Hanna, R. L., and Doudna, J. A. (1997) *Nat. Struct. Biol. 4*, 553−558.
6. Noller, H. F., Hoffarth, V., and Zimniak, L. (1992) *Science 256*, 1416−1419.
7. Hager, A. J., Pollard, J. D., and Szostak, J. W. (1996) *Chem. Biol. 3*, 717−725.
8. Lorsch, J. R., and Szostak, J. W. (1996) *Acc. Chem. Res. 29*, 103−110.
9. Lohse, P. A., and Szostak, J. W. (1996) *Nature 381*, 442−444.
10. Piccirilli, J. A., McConnell, T. S., Zaug, A. J., Noller, H. F., and Cech, T. R. (1992) *Science 256*, 1420−1424.
11. Steitz, T. A., and Steitz, J. A. (1993) *Proc. Natl. Acad. Sci. U.S.A. 90*, 6498−6502.
12. Pyle, A. M. (1993) *Science 261*, 709−714.
13. Dahm, A. C., and Uhlenbeck, O. C. (1991) *Biochemistry 30*, 9464−9469.
14. Dahm, A. C., Derrick, W. B., and Uhlenbeck, O. C. (1993) *Biochemistry 32*, 13040−13045.
15. Chowrira, B. M., Berzal-Herranz, A., and Burke, J. M. (1993) *Biochemistry 32*, 1088−1095.
16. Streicher, B., Westhof, E., and Schroeder, R. (1996) *EMBO J. 15*, 2556−2564.
17. Piccirilli, J. A., Vyle, J. S., Caruthers, M. H., and Cech, T. R. (1993) *Nature 361*, 85−88.
18. Kuimelis, R. G., and McLaughlin, L. W. (1996) *Biochemistry 35*, 5308−5317.
19. Sawata, S., Komiyama, M., and Taira, K. (1995) *J. Am. Chem. Soc. 117*, 2357−2358.
20. Koizumi, M., and Ohtsuka, E. (1991) *Biochemistry 30*, 5145−5150.
21. Zhou, D.-M., Usman, N., Wincott, F. E., Matulic-Adamic, J., Orita, M., Zhang, L.-H., Komiyama, M., Kumar, P. K. R., and Taira, K. (1996) *J. Am. Chem. Soc. 118*, 5862−5866.
22. Pontius, B. W., Lott, W. B., and von Hippel, P. H. (1997) *Proc. Natl. Acad. Sci. U.S.A. 94*, 2290−2294.
23. Smith, D., and Pace, N. R. (1993) *Biochemistry 32*, 5273−5281.
24. Herschlag, D., Piccirilli, J. A., and Cech, T. R. (1991) *Biochemistry 30*, 4844−4854.
25. Chen, Y., Li, X., and Gegenheimer, P. (1997) *Biochemistry 36*, 2425−2438.
26. Sugimoto, N., Kierzek, R., and Turner, D. H. (1988) *Biochemistry 27*, 6384−6392.
27. Sugimoto, N., Tomka, M., Kierzek, R., Bevilacqua, P. C., and Turner, D. H. (1989) *Nucleic Acids Res. 17*, 533−371.
28. Hampel, A., and Cowan, J. A. (1997) *Chem. Biol. 4*, 513−517.
29. Young, K. J., Gill, F., and Grasby, J. A. (1997) *Nucleic Acids Res. 25*, 3760−3766.
30. Suga, H., Lohse, P. A., and Szostak, J. W. (1998) *J. Am. Chem. Soc. 120*, 1151−1156.
31. Ulanovsky, L., Drouin, G., and Gilbert, W. (1990) *Nature 343*, 190−192.
32. Pentz, L., and Thornton, E. R. (1967) *J. Am. Chem. Soc. 89*, 6931−6938.
33. Celander, D. W., and Cech, T. R. (1991) *Science 251*, 401−407.
34. Pyle, A. P., and Cech, T. R. (1991) *Nature 350*, 628−631.
35. Knitt, D. S., and Herschlag, D. (1996) *Biochemistry 35*, 1560−1570.
36. Pyle, A. M., and Green, J. B. (1994) *Biochemistry 33*, 2716−2725.
37. Herschlag, D., and Khosla, M. (1994) *Biochemistry 33*, 5291−5297.
38. Cowan, J. A. (1997) *Inorganic Biochemistry: An introduction*, Wiley-VCH, New York.
39. Burgess, J. (1988) *Ions in solution*, Ellis Horwood Ltd., New York.
40. Jencks, W. P. (1969) *Catalysis in chemistry and enzymology*, McGraw-Hill, New York.
41. Basolo, F., and Pearson, R. G. (1988) *Mechanisms of Inorganic Reactions*, John Wiley & Sons, New York.
42. Black, C. B., Huang, H.-W., and Cowan, J. A. (1994) *Coord. Chem. Rev. 135/136*, 165−202.
43. Black, C. B., and Cowan, J. A. (1994) *J. Am. Chem. Soc. 116*, 253−260.

BI980432A